Chalcogenide Letters Vol. 15, No. 1, January 2018, p. 25 -33

PECULIARITIES OF CRYSTALLIZATION PROCESS FOR $Ge_2Sb_2Te_5$ THIN FILMS BY NANOSECOND SINGLE LASER PULSE

P. LAZARENKO[a*], M. SAVELYEV[a], A. SHERCHENKOV[a], A. GERASIMENKO[a], S. KOZYUKHIN[b,c], V. GLUKHENKAYA[a], A. POLOKHIN[a], Y. SHAMAN[a], A. VINOGRADOV[a]

[a]*National Research University of Electronic Technology, Zelenograd 124498, Russia*

[b]*Kurnakov Institute of General and Inorganic Chemistry, RAS, Moscow 119991, Russia*

[c]*National Research Tomsk State University, Tomsk, 634050, Russia*

Influence of nanosecond single laser irradiation on the surface morphology and structural transformation of the amorphous $Ge_2Sb_2Te_5$ thin films was investigated. The destructions of the $Ge_2Sb_2Te_5$ thin film after single ns pulse laser irradiation with fluence > 99.1 mJ/cm^2 were observed. The laser irradiation with fluence in the range from 74 to 77 mJ/cm^2 leads to crystallization of amorphous phase. Structure of as-deposited, annealed at 180 °C and irradiated thin films were examined by Raman spectroscopy. The intensity and shape of Raman spectra for irradiated (77 mJ/cm^2) and annealed $Ge_2Sb_2Te_5$ thin films are close to each other and correspond to fcc. However, the difference between the Raman spectra of thin film after nanosecond single laser irradiation and literature data for continuous-wave laser were observed.

(Received October 2, 2017; Accepted January 9, 2018)

Keywords: $Ge_2Sb_2Te_5$, Phase change material, Thin film, Laser irradiation, Crystallization

1. Introduction

At this moment, the non-volatile memory devices based on a flash technology are the most widespread among users of the electronic equipment. However, flash memory devices have the low data recording rate, insufficient number of the data recording cycles, low radiation resistance [1]. In this connection chalcogenide semiconductors on the basis of the Ge-Sb-Te system materials are actively investigated nowadays due to their successful commercial application in optical disks (DVD-R/RW, DVD+R/RW and Blu-Ray), and perspectives of their utilization in the electrical non-volatile phase change memory (PCM) devices [2]. However, despite a significant increase of the data recording rate for electric PCM compared to the flash memory, the problem of further increasing the speed of the memory integrated circuits remains actual. The next step on the way of increasing operation rate of electronic devices is introduction of the optical interconnects to the Si integrated microcircuits [3]. Application of the optical interconnections will significantly improve the performance of computers by reducing the delays due to the electrical storage and data processing operations.

A sufficient change in the optical properties of the chalcogenide semiconductor films during phase transformations can be used as the operation principle for fully optical devices including memory ones. Crystallization of the amorphous $Ge_2Sb_2Te_5$ (GST225) thin films under the laser irradiation with nano- and femtosecond duration was demonstrated in the works [4,5]. Short switching time for Ge-Sb-Te thin films by laser beam with a significant change in their optical properties and preservation of the several states including metastable for tens of years [2] open wide perspectives for the application of these materials in the optoelectronic converters (Mach-Zehnder modulators [6]) and fully optical devices [7,8], including high-rate optical memory [9].

*Corresponding author: aka.jum@gmail.com

A considerable number of previous studies have already focused on the crystallization process of PCM materials under isothermal heating and continuous-wave (CW) laser irradiation. In particular, the Raman method was often used for investigation of the structure transformations [10-20]. Results of Raman spectroscopy from various investigations are compiled in Table 1, where RF - radio frequency sputtering, PLD – pulsed laser deposition, TVE - thermal vacuum evaporation, LI – laser irradiation.

Table 1. Literature data on the results of Raman spectroscopy of amorphous and crystalline GST225 thin films

Method of deposition	Amorphous state	Crystalline state		year/ reference/
	Position of peaks, cm^{-1}	Method of crystallization	Position of peaks, cm^{-1}	
RF	151,75	180°C	110, 160	2004 [10]
RF	30, 150	180°C	~120, ~140, 276	2007 [11]
PLD	90, 130, 150, 220,	200÷300°C	105, 130, 150	2009 [12]
Computed model	100, 129, 1 152	Computed model	110, 160	2011 [13]
RF	125, 150	-	-	2012 [14]
TVE	120÷150, 120÷150.	CW LI	110÷145, 145÷160.	2012 [15]
PLD	90, 125, 145, 220.	225÷ 300°C	110, 145, 160, 220	2012 [16]
TVE	80, 125, 153, 300	-	-	2013 [17]
PLD	120-125, 145-150, 215-220	-	-	2016 [18]
TVE	80, 124, 147, 163, 212	CW LI	~90, ~120, ~140	2016 [19]
RF	150	LI	64, 117, 137, 160	2017 [20]

It should be noted, that number and position of determined peaks and their interpretation are different. These differences can be related to many factors including the use of different deposition and crystallization methods. Also, the phase transformation under the short laser irradiation are not sufficiently investigated yet, in particular the results of Raman spectroscopy for GST225 thin films after nanosecond single laser pulse irradiation are practically absent.

The lack of the detailed understanding of phase transformation mechanisms in Ge-Sb-Te thin films under the short laser irradiation is a serious scientific problem. This problem restrains

the development of the physical and technological fabrication principles of the high-rate optical non-volatile memory devices. The decision of this problem will enable purposeful and sufficient improvement of the parameters for the wide range of optical and optoelectronic devices.

So, the aim of this work was investigation of the peculiarities of the influence of nanosecond single laser irradiation on the surface morphology and structural transformation of the $Ge_2Sb_2Te_5$ thin films.

2. Experimental

Thin films of the $Ge_2Sb_2Te_5$ composition were prepared by magnetron sputtering at room temperature. The pressure of Ar during the process was $2 \cdot 10^{-2}$ Torr, the sputtering power was 100 W. The films were deposited on Si substrates (100) after their thermal oxidation. The thicknesses of thin films were controlled by the atomic force microscopy (NT-MDT Solver Pro), and were ~130 nm.

Scanning electron microscope (Philips XL 40) with EDXR spectrometer was used for the microanalysis of the deposited thin films. EDX results showed that composition of as-deposited thin films was close to that of $Ge_2Sb_2Te_5$. The uniform distribution of composition across the thin film thickness was determined by Auger spectroscopy (Perkin Elmer PHI-660).

According to the X-ray diffraction (XRD, Rigaku Smart Lab, step $\Delta\theta = 0.001°$, scanning speed 1° per minute, λ ($CuK_{\alpha 1}$) = 1.5406 Å) as-deposited films were amorphous.

Influence of the power of laser irradiation on the crystallization process in the GST255 films was studied with optical scheme based on the nanosecond pulsed laser (Fig. 1).

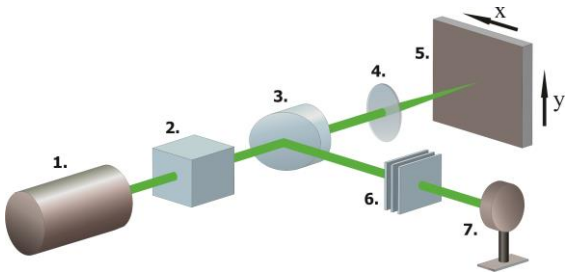

Fig. 1. Optical scheme for irradiation of thin films by laser pulses

Solid-state Nd:YAG laser (JV LOTIS TII LS-2147) (1) was used to generate single laser pulses of the second harmonic at the wavelength of 532 nm with 16 ns duration and linear polarization in the horizontal plane. The polarizing Glan-Taylor prism (2) was added in the optical scheme to adjust the fluence of the beam. When the beam fell on a wedge prism (3) a small part of the energy was removed aside. After the passing through the prism (3) laser radiation was focused by a lens (4) with a focal length of 10 cm and fell on the GST225 film (5) located at a distance of 8 cm behind the lens. The laser beam, allotted by the prism (3) was attenuated by the calibrated neutral set of replaceable filters (6) and then fells on the photodiode energy sensor (Ophir Photonics PD10-C) (7). The sample could be moved along the X and Y axis, perpendicular to the propagation line of the laser radiation.

The shape of the laser beam profile was obtained by using a silicon CCD camera (Spiricon-Ophir Photonics SP620U) with a spectral range of 190-1100 nm. For this purpose, a CCD camera with the resolution of 4.4 μm square pixels was inserted in the place of the sample. The results (Figure 2) showed that the beam profile (dependence of the fluence on the coordinate) of the laser spots have Gaussian distributions.

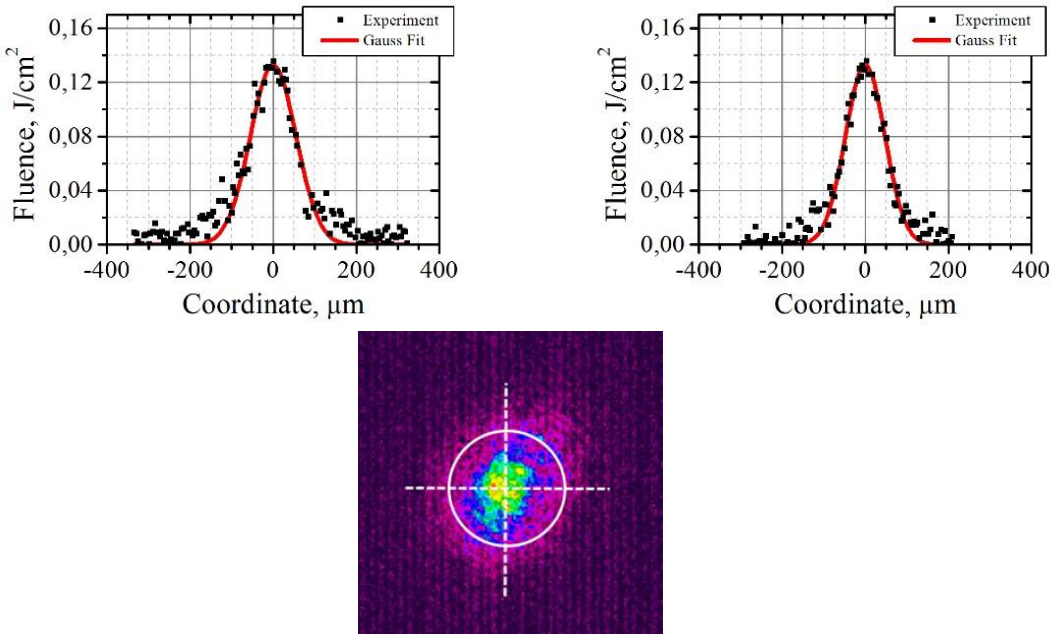

Fig. 2. The beam profile

The incident laser beam was used for the irradiation of the films, and the spot has an elliptical shape with the size of 95 x 110 μm^2. The maximum laser fluence on profile (F_{max}) was varied between 125 and 57 mJ/cm^2.

The Raman spectra of the GST225 samples were obtained with Horiba LabRAM HR Evolution. The He-Ne laser (633 nm, 10 mW) was used as a source of excitation radiation. The diffraction grating 600 lines/mm provided the 1.5 cm^{-1} spectral resolution. The CCD camera was cooled at 200 K for detecting Stokes-side Raman scattering at a wide spectral range. The precision motorized stage and on-board Olympus BX41 microscope were used for the laser beam focusing on the investigated area. The accumulation time and accumulation number were 20 s and 4, respectively. The calibration of the LabRAM HR spectrometer was verified before and after each investigated sample by acquiring Raman spectra of a standard silicon wafer.

Optical microscope (Herox KH-7700), surface profiler (Alpha Step D-120) and scanning electron microscope (SEM, Carl Zeiss NVision 40) were used to investigate morphologies of thin films.

3. Results and discussion

An amorphous GST225 film was irradiated by single ns laser pulses in order to induce an amorphous to crystalline phase transition. Optical images of the thin film surface after excitation by pulses of different fluences are shown in Fig. 3.

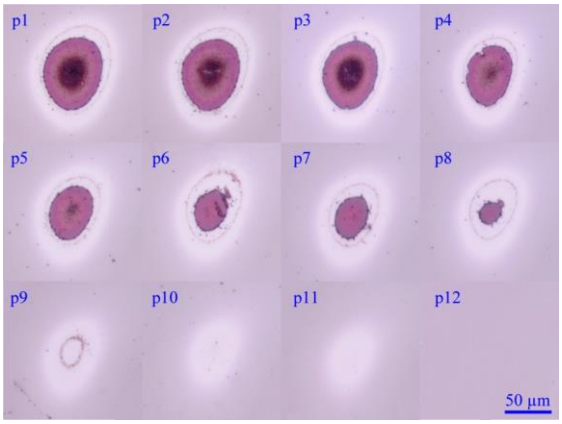

Fig. 3. Optical microscope images of the marks obtained after excitation

Three different ranges of F_{max} may be identified. In the first range (below 57 mJ/cm^2) no changes are observed. In the second range (from 74 to 77 mJ/cm^2) uniform white elliptical marks are formed. In the third range (above 99.1 mJ/cm^2) elliptical marks are uneven and contain different color areas, including the white external and red central regions. The results of the estimation of minor diameter for the white external (D_1) and red central region (D_2) are shown in Table 2. The increase of the laser fluence leads to an increase of the white and red central regions areas.

Table 2. Results of the optical microscopy

Name of mark	p1	p2	p3	p4	p5	p6	p7	p8	p9	p10	p11	p12
F_{max}, mJ/cm^2	125	121	117	109	105	99	98	92	83	77	74	57
D_1, mm	88.6	86	84.4	82.1	84.9	77.1	76.6	72.4	58.1	49.8	48.5	-
D_2, mm	60.0	58.5	56.8	51.7	45.7	33.7	33.2	24.9	-	-	-	-

Investigation of the formed marks morphologies and composition was carried out with the scanning electron microscope, EDXR spectrometer and surface profiler. Morphology and SEM-EDX mapping of Si distribution for p8 and p11 marks are shown in Figure 4.

Significant changes of the morphology in the red central region for the marks after irradiation by the laser pulses with F_{max} > 92 mJ/cm^2 were observed (Fig 4, a). Results of the profilometry showed a sharp drop of profile height in the red region (Fig. 4, b). This change of height is about 125 nm, which corresponds nearly to the thickness of as-deposited GST225 film. So, the red central region of the marks observed by optical microscopy is Si substrate without deposited GST225 thin films.

Results of EDX confirm that red central regions are Si-rich areas compared with the rest of the film surface (Fig 4, c). One of the reasons for this effect can be caused by the local heating due to the laser irradiation, which is accompanied by the appearance of mechanical stresses in the GST225 thin films. These thermal and mechanical perturbations lead to the ablation and destruction of thin film. The initial rupture of the film is confirmed by the peeling, which is observed on the SEM-image of thin film surface (Fig. 4, a). It should be noted, that the increase in the laser fluence leads to the increase in the area of the red central region (Table 2), which may be explained by ablation process.

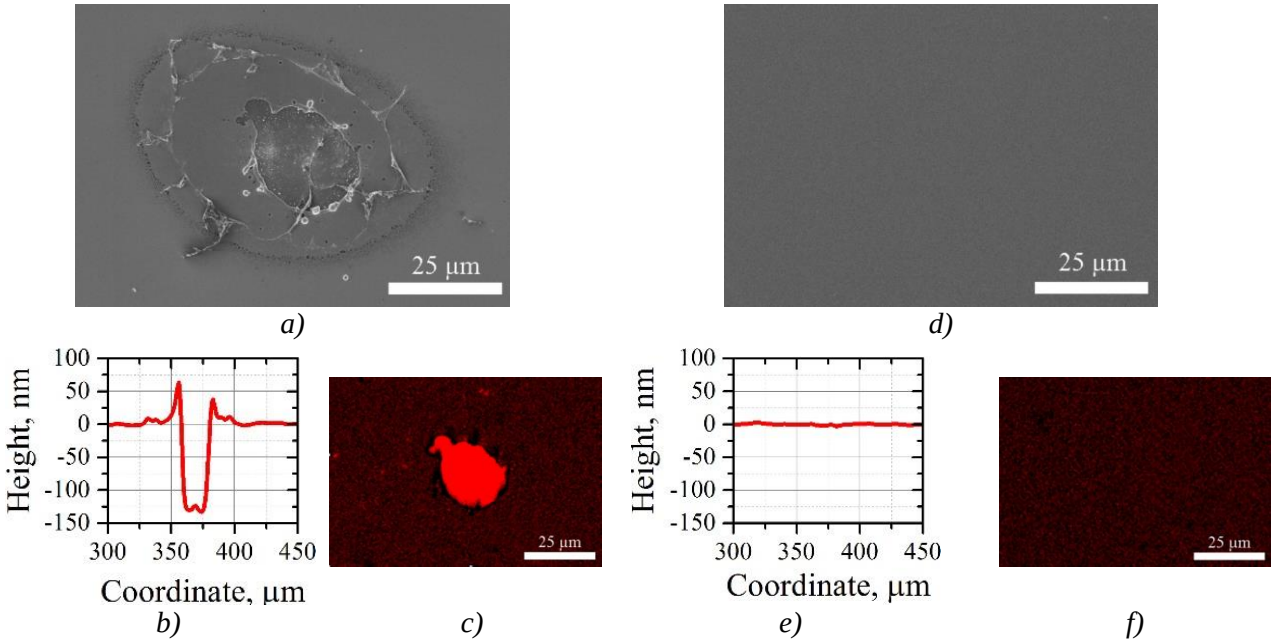

Fig. 4. Results of the investigation: a), d) - SEM pictures; b),e) - height profiles; c), f) - SEM-EDX mapping of Si distribution for p8 and p11 marks, respectively

After excitation by pulses of F_{max} < 77 mJ/cm^2, significant changes in the surface morphologies are not observed (Fig 4, d,e,f). So, the appearance of the white spots on the optical images (Figure 3.2) is due to the change in the optical coefficients of GST225 thin film. The changes in the absorption and reflection coefficients for GST225 can occur due to phase transformations between amorphous and crystalline states [21].

Raman spectroscopy was used to examine the structure of as-deposited thin film and formed marks after the laser irradiation. In this case, the power density irradiated on the sample was kept at the low levels for avoiding strong sample heating and sample structure changes. The laser radiation power was reduced by neutral filters with 1% transmission to approximately 0.1 mW. The excitation laser radiation was focused on the surface of investigated thin films by the 100x objective (diameter of focused spot was 5 µm).

The experimental Raman spectrum of as-deposited GST225 thin film is shown in Fig. 5. Spectrum was measured in the range from 0 to 300 cm^{-1}. The experimental data are close to those for amorphous thin films presented in the works [12,14,18] (Fig. 5, a). The maximum at near 150 cm^{-1} was chosen for normalization, since this peak was found in almost every investigation (Table 1).

The XRD diffraction profile of as-deposited thin film is shown in Fig. 6. Broad peak around 29° is observed. High-resolution transmission electron microscopy was used for checking the structure of as-deposited thin film. The diffuse halo on the diffraction pattern was obtained for as-deposited thin film, which is the evidence of the amorphous phase.

Five main peaks in the spectra with different intensities around 56, 75, 121, 151 and 212 cm^{-1} (Fig, 5, a) were decomposed by Gaussian fitting. It should be noted, that observed peak tail in the low-wavenumber region (under 10 cm^{-1}) is caused by residual Rayleigh scattering.

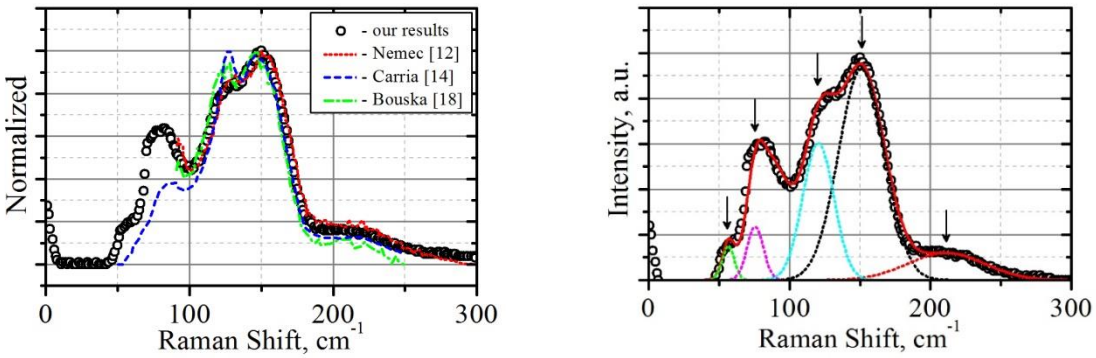

Fig. 5. (Color online) The experimental Raman scattering spectra of amorphous GST225 compared with: a – the results of another authors; b – the results of fitting

The peaks around 125, 150 and 220 cm^{-1} have been reported in many works [12,16,18,19]. A detailed analysis of these peaks is presented in Nemec's paper [16] and is the most convincing. Based on the Raman studies performed on a-GeTe thin films and results of EXAFS, the authors of [16] related vibrations of peak 125 cm^{-1} to the A_1 modes of $GeTe_{4-n}Ge_n$ (n=1, 2) corner-sharing tetrahedra. The peak near 150 cm^{-1} and weak Raman band showing a flat maximum near 220 cm^{-1} were attributed to vibrations A^2_{1g} modes of $SbTe_{3/2}$ and F_2 mode of $GeTe_4$ tetrahedra, respectively. This interpretation is also given in work [19]. However, the low intensity peak at 75 cm^{-1} was identified only in several works [17, 19] and the ending of this peak was recorded in [12, 18]. A paper in which the peak around 56° was described for $Ge_2Sb_2Te_5$ have not found. These peaks can be associated with E and F_2 modes of $GeTe_4$ tetrahedra.

A Raman spectrum measured in the middle of the p11 mark (F_{max} = 77 mJ/cm^2) compared to a spectrum of annealed GST225 thin film are presented in Fig 6. Thermal annealing was carried out at 180 °C for 15 minutes. Such annealing is accompanied by the crystallization of as-deposited film, which was supported by the increasing of the peak intensities in X-ray diffraction patterns (Fig. 7). Analysis of XRD data showed that annealed at 180 °C thin film has a cubic structure. Positions of detected peaks has correlation with the data presented in [22,23].

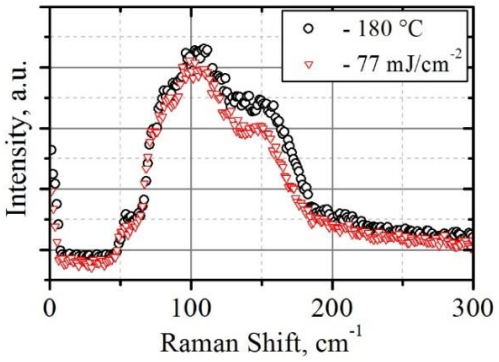

Fig. 6. The Raman scattering spectra of GST225 thin films after annealing and irradiation

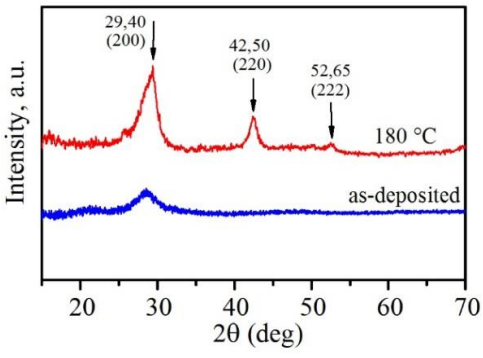

Fig.7. X-ray diffraction patterns for as-deposited and annealed GST225 thin films

The intensity and shape of Raman spectra for both samples are close. On the basis of these results, we concluded that the laser irradiation of F_{max} = 77 mJ/cm^2 leads to crystallization of amorphous phase and the structure of irradiated thin films is close to fcc-GST225. The Raman spectra of these samples have a very broad and complex band in the range 40–250 cm^{-1}, but it

contains at least five peaks. The peaks around 55, 77, 104, 149 and 208 cm^{-1} were decomposed (Fig. 8,a). A peak at ~125 cm^{-1} disappears or it is at least suppressed due to the crystallization. A new peak at ~104 cm^{-1} can be associated to the A_1 mode of $GeTe_4$ corner-sharing tetrahedra [11,16].

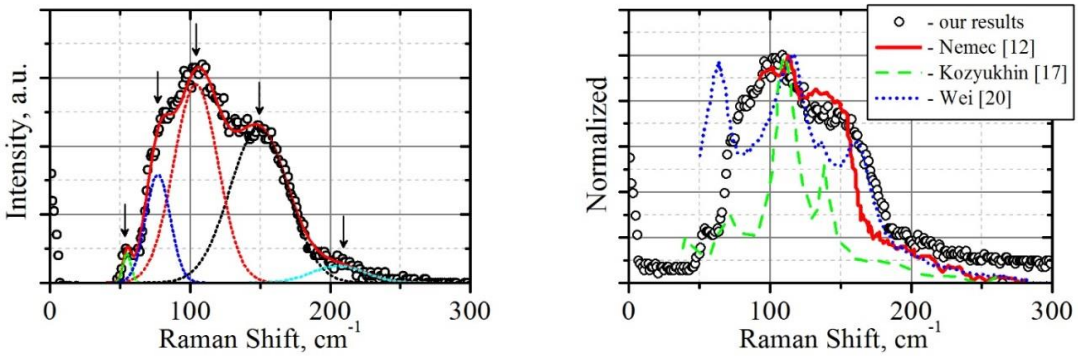

a) *b)*

Fig. 8. (Color online) The experimental Raman scattering spectra of crystalline GST225 film compared with: a – the results of fitting; b – the results of another authors

The experimental Raman spectra are close to results for annealed films presented in [16]. However, it should be noted that our results differ from the data published in the works [17, 20], where a CW laser was used for crystallization. One of the reasons for this might be the differences between the not uniform local heating due to the nanosecond pulsed and continuous-wave laser irradiations [24].

4. Conclusions

Thus, the influence of nanosecond single laser irradiation on the amorphous $Ge_2Sb_2Te_5$ thin films was investigated. The destructions of the $Ge_2Sb_2Te_5$ thin film after single ns pulse laser irradiation with fluences > 99.1 mJ/cm^2 were observed. The reasons for this effect can be caused by the thermal and mechanical perturbations due to the laser irradiation, which are accompanied by ablation and destruction of thin film. The Raman spectra of as-deposited, irradiated and annealed (at 180 °C) $Ge_2Sb_2Te_5$ thin films were analyzed and interpreted. The intensity and shape of Raman spectra for irradiated (77 mJ/cm^2) and annealed (180 °C) $Ge_2Sb_2Te_5$ thin films are close. Analysis of XRD data showed that annealed at 180 °C thin film has a cubic structure. So, the laser irradiation with fluence in the range from 74 to 77 mJ/cm^2 leads to crystallization of amorphous phase. However, our Raman spectroscopy results for the irradiated thin film differ from the data published in the works, where a CW laser was used for crystallization. One of the reasons for this might be the differences between the not uniform local heating due to the nanosecond pulsed and continuous-wave laser irradiations.

Acknowledgements

This study was supported by RFBR (project 17-03-00450), Tomsk State University Competitiveness Improvement Program.

References

[1] D. Liu, L. Yao, L. Long, Z. Shao, Y. Guana, Microprocessors and Microsystems **52**, 343 (2017).
[2] S. Raoux, F. Xiong, M. Wuttig, E. Pop, MRS Bulletin **39**(8), 703 (2014).
[3] C. Sun, M. T. Wade, Y. Lee, J. S. Orcutt, L. Alloatti, M. S. Georgas et.al., Nature **528**, 534 (2015).
[4] Y. Liu, M. M. Aziz, A. Shalini, C. D. Wright and R. J. Hicken, Journal of Applied Physics **112**, 123526 (2012).
[5] X. Sun, M. Ehrhardt, A. Lotnyk, P. Lorenz, E. Thelander, J. W. Gerlach, T. Smausz, U. Decker, B. Rauschenbach, Scientific Reports **6**, 1 (2016).
[6] H. Liang, R. Soref, J. Mu, A. Majumdar, X. Li, W. Huang, Journal of Lightwave Technology **33**(9), 1805 (2015).
[7] M. Stegmaier, C. Rios, H. Bhashkaran, C. D. Wright, W. H.P. Pernice, Adv. Optical Mater **5**(1), 1600346 (2016).
[8] T. Moriyama, D. Tanaka, H. Kawashima, M. Kuwahara, X. Wang, H, Tsuda, IEICE Electronics Express **11**(15), 1 (2014).
[9] C. Rios, M. Stegmaier, P. Hosseini, D. Wang, T. Scherer, C. D. Wright, H. Bhaskaran, W. H. P. Pernice, Nature Photonics **9**, 725 (2015).
[10] L. Boy, S. Ting, F. Song-Lin, C. Bomy, Chinese Physics **13**(11), 1947 (2004).
[11] K.S. Andrikopoulos, S.N. Yannopoulos, A.V. Kolobov, P. Fons, J. Tominaga, Journal of Physics and Chemistry of Solids **68**, 1074 (2007).
[12] P. Nemec, A. Moreac, V. Nazabal, M. Pavlišta, J. Přikryl, M. Frumar, Journal of Applied Physics **106**, 103509 (2009).
[13] G. C. Sosso, S. Caravati, R. Mazzarello,M. Bernasconi, Physical Review **83**, 134201 (2011).
[14] E. Carria, A. M. Mio, S. Gibilisco, M. Miritello, F. d'Acapito, M. G. Grimaldi, E. Rimini, Electrochemical and Solid-State Letters, **14**(12), 480 (2011).
[15] A. P. Avachev, S. P. Vikhrov, N. V. Vishnyakov, S. A. Kozyukhin, K. V. Mitrofanov, E. I. Terukov, Semiconductors **46**(5), 591 (2012).
[16] P. Nemec, V. Nazabal, A. Moreac, J. Gutwirth, L. Benes, M. Frumar, Materials Chemistry and Physics **136**, 935 (2012).
[17] S. Kozyukhin, M. Veres, H. P. Nguyen, A. Ingram, V. Kudoyarova, Physics Procedia **44**, 82 (2013).
[18] M. Bouška, S. Pechev, Q. Simon, R. Boidin, V. Nazabal, J. Gutwirth, E. Baudet, P. Němec, Scientific Reports **6**, 26552 (2016).
[19] S. Kozyukhin, Yu. Vorobyov, A. Sherchenkov, A. Babich, N. Vishnyakov, O. Boytsova, Physica Status solidi A **213**(7), 1831 (2016).
[20] T. Wei, J. Wei, K. Zhang, H. Zhao, L. Zhang, Scientific Reports **7**, 42712 (2017).
[21] S. Kozyukhin, A. Sherchenkov, A. Babich, P. Lazarenko, H.P. Nguyen, O. Prikhodko, Canadian Journal of Physics **92**, 684 (2014).
[22] D. Lee, S.S. Lee, W. Kim, C. Hwang, Applied Physics Letters **91**(25), 251901 (2007).
[23] G. Zhang, D. Gu, F. Gan, X. Jiang, Q. Chen, Thin Solid Films **474**, 169 (2005).
[24] J. K. Behera, X. Zhou, J. Tominaga, R. E. Simpson, Optical Materials express **7**(10), 3741 (2017).